Supporting information

Raman and autofluorescence spectroscopy for in situ identification of neoplastic tissue during surgical treatment of brain tumors

Ortrud Uckermann, Jonathan Ziegler, Matthias Meinhardt, Sven Richter, Gabriele Schackert, Ilker Y. Eyüpoglu, Mido M. Hijazi, Dietmar Krex, Tareq A. Juratli, Stephan B. Sobottka, Roberta Galli

Methods

Patients

Table S1 Number of patients and of acquired spectra.

Ex vivo measurements		
Tissue type	**n. of patients**	**n. of spectra**
Non-neoplastic	4	39
GBM	20	89
Metastases	11 ♦	52
Meningioma	13 †	195
Total	48	375

In situ measurements		
Tumor type	**n. of patients**	**n. of spectra**
Glioma WHO II-III	6 ‡	45
GBM	10	75
Metastases	10 ♣	86
Meningioma	3	12
Total	29	218

♦ Lung n=4, breast n=1, digestive tract n=3 and squamous cell carcinoma n=2, melanoma n=1

† Associated dura available for n=4 patients (n=41 spectra)

‡ Astrocytoma n = 3, oligodendroglioma n = 3

♣ Lung n=5, breast n=2, colorectal n=1 and squamous cell carcinoma n=1, melanoma n=1

Raman probe and spectrometer

The spectrometer and laser source are connected to the probe via a Y-piece using fiber optic fibers, so that excitation and detection can be realized coaxially through the probe. For this purpose, the cylindrical tip of the probe, which has a diameter of 2.1 mm, is equipped with a two-component lens with a diameter of 2 mm at the front end. The probe is designed for immersion or direct contact measurement. The laser-guiding 300 µm-core low-hydroxyl (OH) fiber with a numerical aperture (NA) of 0.22 is located in the center of the probe. A narrow bandpass filter centered on the laser wavelength is located at the front end. Seven identical 300 µm-core low-OH fibers (NA=0.22) surround the excitation fiber and collect the inelastic Raman scattering as well as the spectrally superimposed near-infrared autofluorescence. A high-pass filter in front of the collecting fibers blocks the elastic Rayleigh scattering.

The transmission holographic Raman spectrometer type HT from EmVision includes the spectrograph, as well as a CCD camera (DU420A-BR-DD, Andor Technology Ltd., Belfast, UK) operated at a temperature of -60 °C. The system is equipped with an optical filter with optical density > 6 at 785 nm to reject all residual elastically scattered light that was not filtered by the probe. The spectral range of the spectrometer is 350 - 2100 cm^{-1} (or 807 - 940 nm given as wavelength). The f-number is f/2.2 and

the slit aperture size is 50 µm. The CCD camera is connected to a PC via USB interface. The Solis software (Andor Technology Ltd., Belfast, UK) was used to set the acquisition and to record the spectra. The spectrum of acetaminophen was used for system spectral calibration, which was performed following the manufacturer's protocol.

Histology and immunohistochemistry

All samples were fixed in 4% formaldehyde solution at 7 °C for 1-5 days and freeze-protected in ascending sucrose solution (10% and 30% for 24 h each). Samples were embedded in cryomedium, frozen on dry ice and then stored at -80 °C. Frozen tissue sections were prepared with a thickness of 10 µm and stored at -20 °C until staining.

Hematoxylin and eosin staining: The sections were washed in aqua dest and incubated in Meyer's hematoxylin/hemalum for 3 min. After washing in distilled water, the tissue was briefly destained in HCl-ethanol. Washing using tap water for 5 min was followed by 3 min staining in eosin (1% eosin G in 80% ethanol). The sections were dehydrated in rising ethanol concentrations, cleared in xylene and coverslipped using Entellan.

Ki67 staining: Tissue sections were allowed to thaw for 20 minutes at room temperature, fixed with a methanol-acetone solution at -20°C, and then dried for 30 minutes. For heat-induced epitope recovery, cryosections were incubated in a citrate buffer (pH=6.0) for 20 min in a steamer. Peroxidase blocking was performed with 0.3% hydrogen peroxide-methanol solution for 10 min. The block serum was added (0.3% TritonX in 1% bovine serum albumin solution) followed by 1 h incubation. The primary antibody (Novocastra monoclonal mouse antibody Ki67 antigen, Leica Biosystems) was then added to the block serum (1:200) and sections were incubated for 1 h. After washing with PBS, the sections were incubated with the secondary antibody (Histofine Simple Stain MAX PO (M), Nichierei Biosciences) followed by colorimetric detection of the antibody signal (HistoGreen Kit, Linaris). After washing again with PBS, counterstaining with nuclear red was performed. Finally, the sections were dehydrated in ethanol and xylene, and coverslipped with Entellan. For each staining series, a positive control with histological reference material and a negative control without addition of the primary antibody were performed.

Spectral preprocessing and correction of artefacts

After recording, the tissue raw spectra containing both fluorescence signal and Raman spectrum, as well as background spectra, were exported as ASCII files and further processed using standard function in MatLab 2021b (The MathWorks, Inc., Natick, MA, USA).

First, the background was subtracted from the tissue raw spectrum, and then the obtained tissue spectra were reduced to the spectral range 366 - 2043 cm^{-1} to remove artefacts at the edges of the detection window (Fig. S1 a solid lines). To separate the fluorescence and Raman signals, a baseline was calculated using the MatLab function "msbackadj". For this, a double linear interpolation was chosen as the regression method to determine the baseline with a window and step size of 100 cm^{-1} each. The baseline curve represents the fluorescence (Fig. S1 a, dashed lines). The baseline curve was then subtracted from the spectra to retrieve the Raman spectrum (Fig. S1 b, dotted lines). Subsequently, the spectral range was reduced to 472 - 2009 cm^{-1} to remove baseline artefacts at the spectral edges.

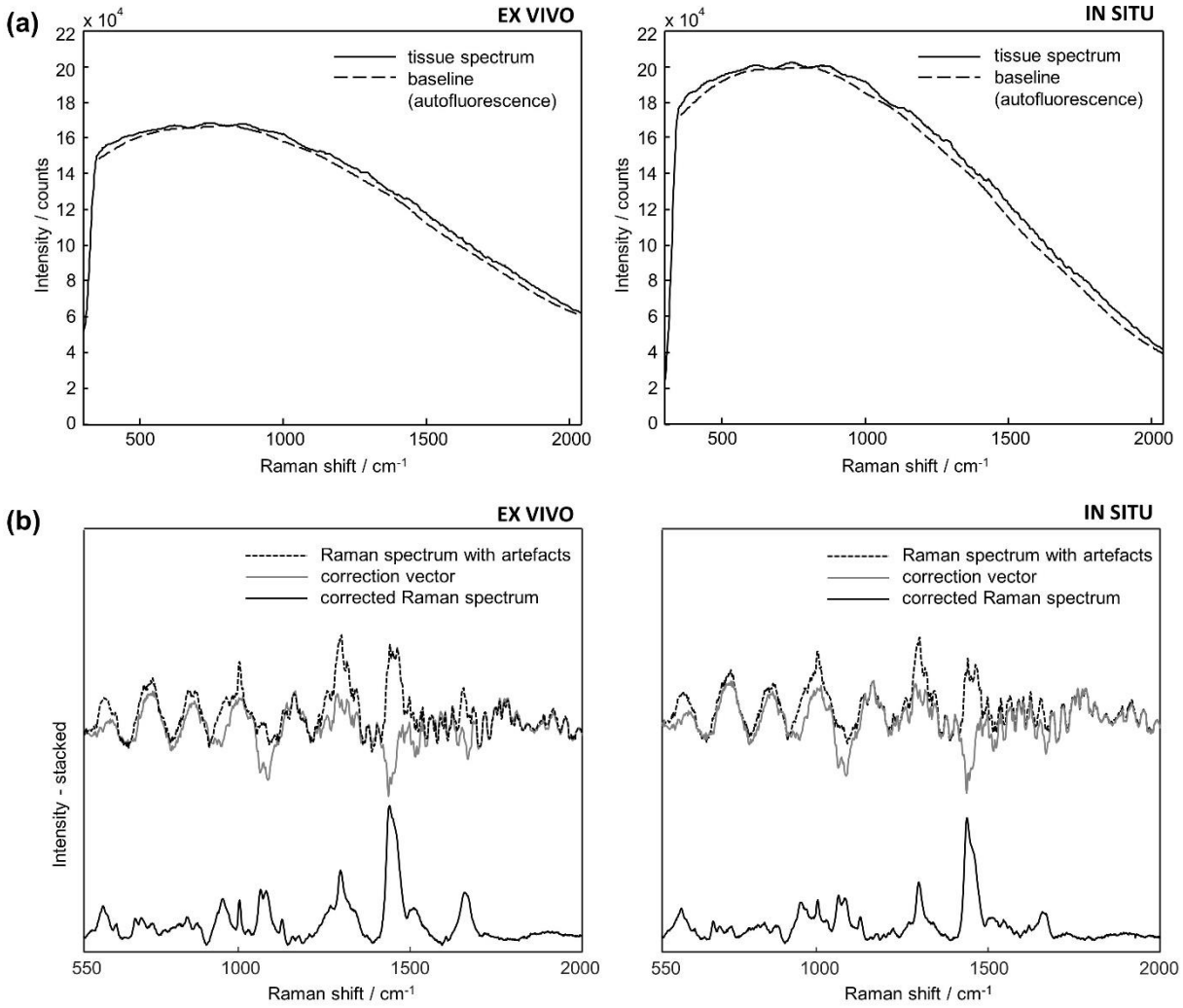

Fig. S1 Pre-processing of spectra. (a): mean raw tissue spectra acquired ex vivo and in situ (solid line) and retrieved baseline (i.e., fluorescence) curve (dashed line) line. (b): Correction of Raman spectra for elimination of spectrometer artefacts: the mean Raman spectrum of ex vivo and in situ measurements are shown before artefact correction (dotted black line) overlaid with the correction vector (grey line) that was multiplied by the mean value of the correction coefficient ($c_{ex\ vivo}$ = 1.27; $c_{in\ situ}$ = 1.44); the corrected Raman spectrum is the solid black line.

Raman spectra obtained after preprocessing were affected by artefacts superimposing to the Raman bands. These artefacts depend from the amount of light entering the spectrometer and/or incoming on the CCD. In case of brain samples, which are characterized by a high fluorescence and weak Raman signal, they completely obscure the Raman bands. An algorithm for correction was then developed as follows.

A preliminary series of measurement was performed on 18 human and 2 murine fresh tissue samples leading to acquisition of total of 444 spectra (108 spectra of mouse brain, 112 spectra of normal human brain from epilepsy surgery, and 224 spectra of human brain tumors). Principle component analysis ("pca" function of Matlab) was applied to the spectra after preprocessing as described above. The second principal component fully described the artefacts (Fig. S1 b, grey lines), and the corresponding eigenvector (v) was used for correction. In order to adapt it to the individual artifact amplitude of each spectrum, a coefficient (c) was calculated for the spectral range devoid of Raman bands between 1727

and 2009 cm^{-1} using the method of least squares, so that the residual square sum between the respective uncorrected spectrum (y_0) and the correction vector is minimal. The difference of spectrum and product of the coefficient and correction vector gives the artifact-corrected spectrum (y_1):

$$y_1 = y_0 - c \cdot v$$

The corrected Raman spectra (Fig. S1 b, solid lines) make it possible to interpret the band pattern. The spectra used to retrieve the correction vector are consistent with the spectra acquired ex vivo as well as in vivo, so that this correction approach works well on all data.

After correction, Raman spectra were vector normalized before proceeding with further analysis and classification.

Development of the classification model

Only Raman and autofluorescence spectra of normal brain tissue and of tumors measured ex vivo (i.e., excluding spectra of dura) were used to build the training set for classification. Principal component analysis (PCA) on Raman and fluorescence spectra of ex vivo measurements was performed using the Matlab function "pca". The PCA coefficients of Raman and autofluorescence datasets were handed over to discriminant analysis for classification in two groups, i.e., normal tissue and neoplastic tissue. The discriminant analysis was performed with the Matlab function "classify". Leave-one out cross validation was used in order to define the type of discriminant function (i.e., linear or quadratic) and the number of principal components to be used in order to maximize classification performances. For instance, K-fold leave-one-out cross-validation was used for estimation of performances, with K equal to the number of patients (i.e., leave-one-patient-out cross-validation).

For Raman data, a cross validation correct rate of 0.8623 (sensitivity = 0.8475, specificity = 0.9744) was achieved using the first ten coefficients (which explain 75.4% of variability) and linear discriminant analysis. For autofluorescence data, best classification in the cross-validation was achieved again with linear discriminant analysis but using just the first three PCA coefficients. The correct rate of cross-validation was 0.9251, with sensitivity = 0.9322 and specificity = 0.8718. The eigenvectors of the principal components used for classification are shown in Fig. S2. Classification results of cross validation of autofluorescence and Raman training data sets are described in the Results' section of this Supporting Information. The data set acquired in situ was classified using the ex vivo data as training set. Therefore, the PCA coefficients of in situ Raman and fluorescence data sets were retrieved based on eigenvectors of the corresponding ex vivo data sets and then classified with the model developed on the ex vivo data sets.

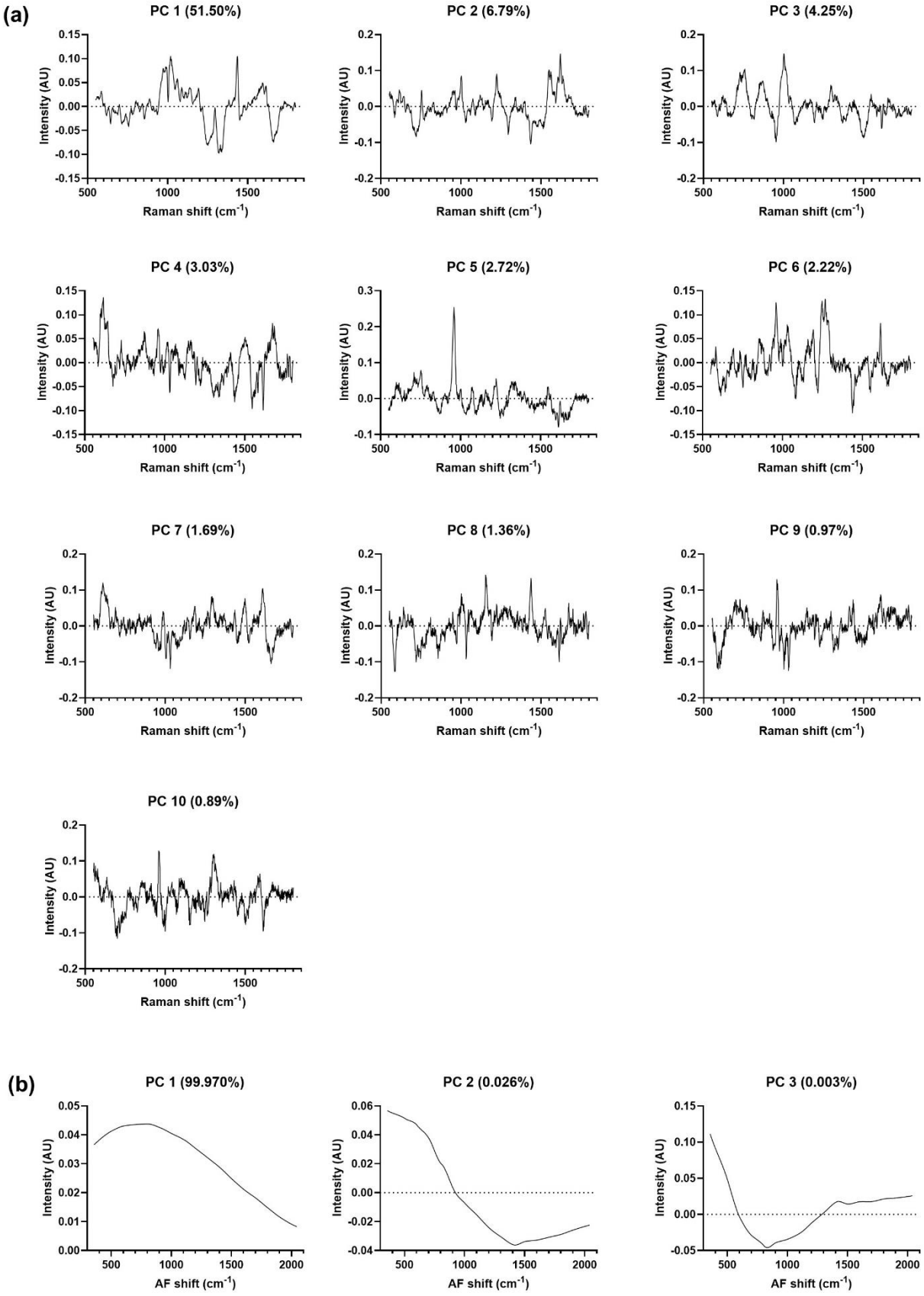

Fig. S2 Principal component analysis. (a): Eigenvectors of first ten components of the Raman dataset; (b): eigenvectors of the first three components of the autofluorescence dataset. The percentage given in parenthesis is the variance explained by each component.

Results

Spectroscopy of ex vivo human samples

Spectra were acquired from resected fresh samples of brain tumors and hippocampi of epileptic patients. Mean Raman spectra (retrieved after preprocessing and spectrometer artefact correction of each single spectrum, Fig. S3 a) show differences among tissue types. Spectral variations of overlapping bands can be appreciated in difference spectra, which are obtained by subtracting the mean Raman spectrum of non-neoplastic brain from the mean Raman spectra of each tumor type (Fig. S3 b). These differences are resumed by the protein band 1240-1280 cm^{-1} (amide III vibration) and the lipid band at 1437 cm^{-1} (deformation vibration of CH_2 groups). The dura contains more proteins and less lipids than both brain tissue and meningioma. Therefore, the Raman spectrum of meningioma is different compared to non-neoplastic brain as well as to the dura from which it originates.

Autofluorescence intensity is shown in Fig. S3 c. The median autofluorescence intensity of non-neoplastic brain tissue is higher than the one of all tumor types and of dura, and significant differences exist among medians of the five tissue types (Kruskal-Wallis test, $P < 0.001$). However, the scattering of the single values, as well as the overlap among tissue type is high.

The information carried by Raman spectra and autofluorescence intensity are linked (Fig. S3 d,e). Autofluorescence intensity correlates positively with the intensity of the Raman band at 1437 cm^{-1} (Spearman $r = 0.86$, $P < 0.001$) and correlates negatively with the intensity of amide III spectral feature at 1240-1280 cm^{-1} (Spearman $r = -0.84$, $P < 0.001$).

Classification of ex-vivo data

The classification results from the cross validation of the Raman and autofluorescence training sets are shown for each spectrum and patient in Fig. S4. The intensities of autofluorescence, as well as of lipids and proteins Raman bands (1437 cm^{-1} and 1240-80 cm^{-1}, respectively) are given as reference to help interpreting the classification results.

In the comparison of reclassification based on Raman spectra and autofluorescence, it can be seen that Raman spectroscopy is best for recognition of non-neoplastic brain tissue, while autofluorescence provides better results especially for recognition of gliomas and glioblastomas. However, in case of samples with many misclassified spectra, these were wrong classified by both approaches (e.g., non-neoplastic sample of patient 1, glioma/GBM samples of patients 16 and 19, as well as metastatic samples of patients 1 and 11). Furthermore, spectra that were wrongly classified based on Raman data typically display an intensity of lipid and amide III band that are similar to non-neoplastic tissue, while spectra that are misclassified based on autofluorescence display high autofluorescence intensity similarly to normal tissue. It has to be noted that several tumor spectra with high lipid content and low protein band intensities were nevertheless correctly classified: this is explained by the fact that several principle components were used for classification, which resulted consequently based on more spectral features reflecting additional biochemical alterations.

Tumor patients whose samples were more often wrongly classified are the GBM n. 10, 13, 16 and 19, and the metastases n. 1 and 11. Retrospective histopathological evaluation of the tissue of these samples showed that in two cases the GBM tissue was necrotic (n. 13 and 16), in two cases a border region with normal tissue or with very few tumor cells (n. 10 and 19). For metastases, the sample of the patient n.1 resulted to be a border region of normal tissue, while that sample of the patient n. 11 was not assessable.

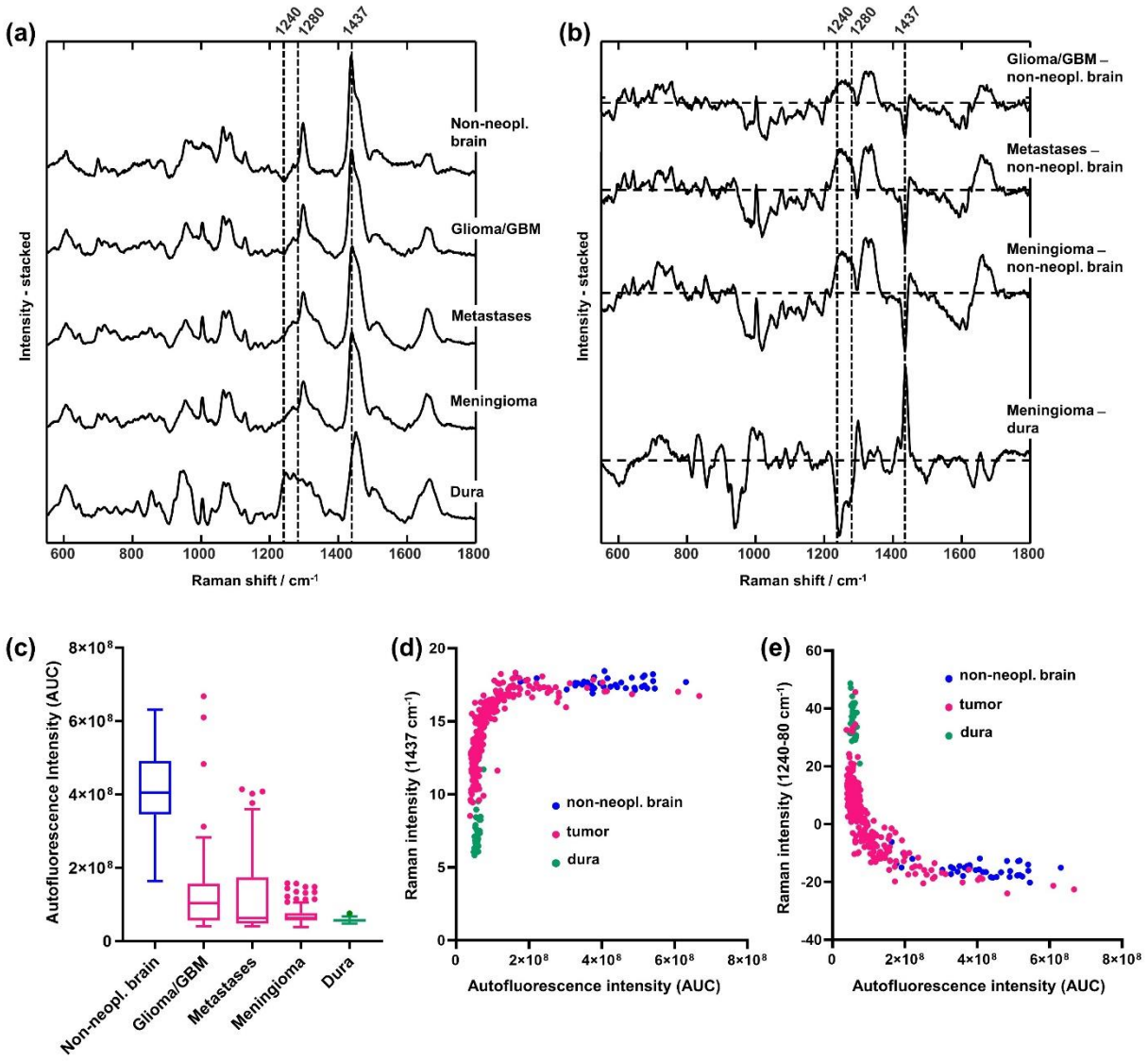

Fig. S3 Spectroscopy of ex vivo tissue samples. (a): mean Raman spectra. (b): mean difference spectra of tumors and non-neoplastic brain tissue. (c): autofluorescence intensity; the value of each measurements are reported with the median for each group. (d): scatter plot of autofluorescence intensity and intensity of the Raman band of lipids at 1437 cm^{-1}. (e): scatter plot of autofluorescence intensity and intensity of the Amide III protein Raman band between 1240 and 1280 cm^{-1}.

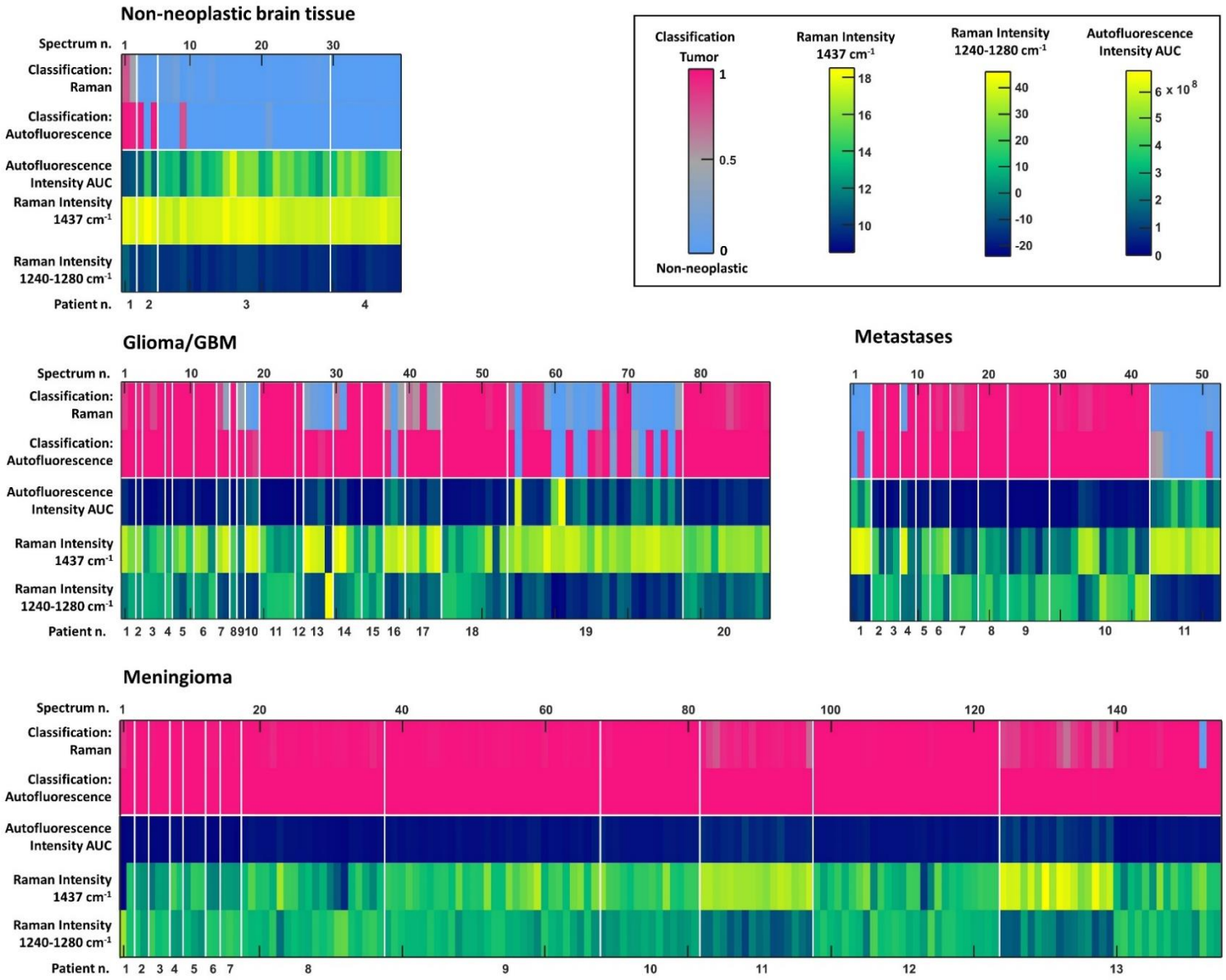

Fig. S4 Reclassification of ex vivo tissue samples. Reclassification results (training set) are shown for each spectrum of each patient split for tissue type. Each vertical strip represents a spectrum and the color codes classification results as well as intensities of Raman bands at 1437 cm^{-1} (lipids) and 1240-1280 cm^{-1} (amide III) and autofluorescence intensity. White lines separate groups of spectra of each patients.